

Arteriosclerosis, Thrombosis, and Vascular Biology

JOURNAL OF THE AMERICAN HEART ASSOCIATION



Calcification by Valve Interstitial Cells Is Regulated by the Stiffness of the Extracellular Matrix

Cindy Ying Yin Yip, Jan-Hung Chen, Ruogang Zhao and Craig A. Simmons
Arterioscler. Thromb. Vasc. Biol. 2009;29:936-942; originally published online Mar 19, 2009;

DOI: 10.1161/ATVBAHA.108.182394

Arteriosclerosis, Thrombosis, and Vascular Biology is published by the American Heart Association,
7272 Greenville Avenue, Dallas, TX 75214

Copyright © 2009 American Heart Association. All rights reserved. Print ISSN: 1079-5642. Online
ISSN: 1524-4636

The online version of this article, along with updated information and services, is
located on the World Wide Web at:

<http://atvb.ahajournals.org/cgi/content/full/29/6/936>

Data Supplement (unedited) at:

<http://atvb.ahajournals.org/cgi/content/full/ATVBAHA.108.182394/DC1>

Subscriptions: Information about subscribing to Arteriosclerosis, Thrombosis, and Vascular
Biology is online at

<http://atvb.ahajournals.org/subscriptions/>

Permissions: Permissions & Rights Desk, Lippincott Williams & Wilkins, a division of Wolters
Kluwer Health, 351 West Camden Street, Baltimore, MD 21202-2436. Phone: 410-528-4050. Fax:
410-528-8550. E-mail:

journalpermissions@lww.com

Reprints: Information about reprints can be found online at

<http://www.lww.com/reprints>

Calcification by Valve Interstitial Cells Is Regulated by the Stiffness of the Extracellular Matrix

Cindy Ying Yin Yip, Jan-Hung Chen, Ruogang Zhao, Craig A. Simmons

Objective—Extensive remodeling of the valve ECM in calcific aortic valve sclerosis alters its mechanical properties, but little is known about the impact of matrix mechanics on the cells within the valve interstitium. In this study, the influence of matrix stiffness in modulating calcification by valve interstitial cells (VICs), and their differentiation to pathological phenotypes was assessed.

Methods and Results—Primary porcine aortic VICs were cultured in standard media or calcifying media on constrained type I fibrillar collagen gels. Matrix stiffness was altered by changing only the thickness of the gels. Calcification did not occur in standard media, regardless of matrix stiffness. However, when VICs were grown in calcifying media on relatively compliant matrices with stiffness similar to that of normal tissue, they readily formed calcified aggregates of viable cells that expressed osteoblast-related transcripts and proteins. In contrast, VICs cultured in calcifying media on stiffer matrices (similar to stenotic tissue) differentiated to myofibroblasts and formed calcified aggregates that contained apoptotic cells. Actin depolymerization reduced aggregation on stiff, but not compliant, matrices. TGF- β 1 potentiated aggregate formation on stiff matrices by enhancing α -smooth muscle actin expression and cellular contractility, but not on compliant matrices attributable to downregulation of TGF- β receptor I. Cell contraction by VICs inhibited Akt activation and enhanced apoptosis-dependent calcification on stiff matrices.

Conclusions—Differentiation of VICs to pathological phenotypes in response to biochemical cues is modulated by matrix stiffness. Although osteogenic or myofibroblastic differentiation of VICs can result in calcification, the processes are distinct. (*Arterioscler Thromb Vasc Biol.* 2009;29:936-942.)

Key Words: aortic valve ■ matrix mechanics ■ mechanobiology ■ collagen ■ sclerosis

Dysregulation of normal cellular processes^{1,2} leads to aortic valve sclerosis (AS), a common disease³ that involves chronic inflammation, fibrosis, and calcification.^{4,5} The consequences of AS are serious, as even minor valve calcification increases the risk of other cardiovascular disorders by 50%, and the prognosis with progression to sclerosis is poor.⁶ Treatment is limited to surgical replacement of the stenotic valves, as effective medical therapies do not exist.

The progression of sclerosis and calcification is mediated primarily by valve interstitial cells (VICs) that populate the interstitial matrix.^{1,7} As in the vasculature,⁸ calcification of the aortic valve occurs through multiple mechanisms,⁹ including apoptosis-related calcification typically associated with myofibroblastic activation of VICs,^{10,11} calcium deposition associated with necrotic cells,¹² and bone formation by resident VICs¹³ or bone marrow-derived cells.¹⁰ However, details of the cellular mechanisms by which VICs contribute to calcification are not well understood, largely because of the limited number of studies in vitro and difficulties with their interpretation. For example, when VICs are induced to form

calcified multicellular aggregates in vitro, the aggregates are associated with the expression of bone-related transcripts and proteins, the expression of myofibroblast markers, or apoptosis.^{7,14–17} It is unclear whether these features represent a single or multiple calcification process(es).

The factors that contribute to the dysregulation of VICs leading to calcification are also not fully defined. While a variety of biochemical cues, including transforming growth factor (TGF)- β , have been implicated in valve calcification,⁵ mechanical cues from the extracellular matrix may also regulate cell function, both in vivo and in vitro. Notably, cells are able to “sense” the local mechanical properties of their extracellular matrix, and matrix stiffness is known to regulate motility, proliferation, and differentiation in various cell types.¹⁸ The differentiation of VICs to myofibroblasts was recently shown to be influenced by matrix stiffness,¹⁹ but the role of matrix mechanics in regulating calcification by VICs has yet to be determined. An improved understanding of VIC-matrix interactions is required to aid in interpretation of VIC calcification studies in vitro; to guide

Received June 10, 2008; revision accepted March 5, 2009.

From the Institute of Biomaterials and Biomedical Engineering (C.Y.Y.Y., J.-H.C., R.Z., C.A.S.), Cardiovascular Sciences Collaborative Program (C.Y.Y.Y.), the Department of Mechanical and Industrial Engineering (J.-H.C., C.A.S.), and the Faculty of Dentistry (C.A.S.), University of Toronto, ON, Canada.

Correspondence to Craig A. Simmons, Department of Mechanical & Industrial Engineering, University of Toronto, 5 King’s College Road, Toronto, ON, Canada M5S 3G8. E-mail c.simmons@utoronto.ca

© 2009 American Heart Association, Inc.

Arterioscler Thromb Vasc Biol is available at <http://atvb.ahajournals.org>

DOI: 10.1161/ATVBAHA.108.182394

the selection of biomaterials with appropriate mechanical properties for valve tissue engineering; and to assess whether alterations in extracellular matrix mechanics that occur with disease^{20,21} modulate pathological changes in VIC phenotypes and calcification processes.

To gain a better understanding of calcification by VICs and its regulation by mechanical cues, we studied the influence of matrix stiffness on primary porcine aortic VICs in vitro using a fibrillar collagen-based system with tunable substrate stiffness. We found that the response of VICs to procalcific soluble factors is sensitive to matrix stiffness. VICs grown in procalcific conditions preferentially differentiate to osteoblast-like cells on compliant substrates that mimic the stiffness of normal or early sclerotic tissue, but differentiate to myofibroblasts on stiffer substrates that mimic the stiffness of stenotic tissue. Calcified aggregates form in both cases, but through distinct processes that are differentially mediated by cytoskeletal tension.

Methods

Valve Interstitial Cell Culture

Primary porcine aortic VICs were isolated by collagenase digestion. Constrained compliant and stiff collagen matrices were constructed following procedures described previously.²² The stiffness was controlled by changing only the thickness of the matrices, which were otherwise formed identically. VICs were seeded on collagen matrices in either DMEM with 10% fetal bovine serum (FBS), or in calcifying medium consisting of complete medium supplemented with 10 mmol/L β -glycerophosphate, 10 μ g/mL ascorbic acid and 10 nmol/L dexamethasone.

Characterization of Collagen Content and Mechanical Properties of Collagen Matrices

Collagen content and the effective stiffness of the compliant and stiff matrices throughout the culture period were measured by the hydroxyproline assay and compression testing, respectively. The effective stiffness of the matrices was also estimated under shear loading by finite element analysis (please see the supplemental materials, available online at <http://atvb.ahajournals.org>).

Cellular Proliferation and Viability

Proliferation of VICs was determined based on measurement of DNA content. Cell viability was determined by fluorescent labeling of live cells with calcein AM and of dead cells with ethidium homodimer-1 (EthD-1). Apoptotic cells were identified by cellular uptake of APOPercentage dye (Bicolor Ltd).

Osteoblast-Related Biomarkers

Transcriptional expression of osteonectin and osteocalcin were quantified by real-time PCR. The amount of the bone transcription factor runt-related transcription factor 2 (Runx2) was measured in VIC nuclear extracts using an ELISA-based immunoassay (TransAM kit, ActiveMotif) and normalized by total cell number. Alkaline phosphatase (ALP) activity was detected by biochemical staining. Osteocalcin was detected by immunohistochemical staining. VIC cultures were stained with Alizarin red S (ARS) solution for calcium deposition. Calcium content was quantified by measuring the absorbance of ARS dye released from the stained culture.²³

Immunofluorescent Staining of Cytoskeletal Proteins

VICs were fixed and permeabilized for costaining with monoclonal mouse anti- α -smooth muscle actin antibody (α -SMA) and fluorescein isothiocyanate (FITC)-conjugated Phalloidin for F-actin followed by nuclear counterstain with Hoechst 33242 dye.

Disruption of Cytoskeleton Assembly and TGF- β 1 Response

VICs were cultured on compliant or stiff matrices with calcifying media for 6 days, at which point aggregation had not occurred on either matrix. VICs were then treated with 0.4 nmol/L swinholide A (SWA) for 2 days to disrupt the assembly of actin. In a separate set of experiments, VICs were cultured on compliant and stiff matrices and were treated immediately with calcifying media (containing 10% FBS) and 5 ng/mL of TGF- β 1 for 5 days to induce α -SMA-dependent aggregate formation.

Secreted TGF- β 1 and TGF- β 1 Receptor Expression

The total amount of TGF- β 1 in supernatant collected from cultured cells was measured and normalized to total cell number. Transcriptional expression of TGF- β 1 receptor I and receptor II were estimated by RT-PCR.

Contraction-Dependent Apoptosis and Akt Activation

A stress-relaxation collagen gel model²⁴ was used to evaluate the relationship between cell contraction, apoptosis, and Akt activity. Briefly, VICs were cultured on the surface of constrained collagen gels for 6 days, at which point the gels were released. Apoptosis was measured immediately as well as 0.5 hours and 3 hours after gel release. Total and phosphorylated Akt were detected in cell lysates before and 1 hour after gel release by Western blotting.

Statistical Analysis

Results are presented as mean \pm SE. Unpaired Student *t* test or ANOVA and Fisher least significant difference test were used as appropriate.

Results

Characterization of Collagen Matrices

Cells were cultured on constrained fibrillar collagen matrices. Thick (\approx 2.5 mm thickness) and thin (\approx 10 μ m thickness) matrices had uniform fibrillar collagen microstructure (supplemental Figure IA and IB), with similar collagen fiber diameters ($P=0.27$, supplemental Figure IC). Because of the differences in the gel thickness alone, the thick matrices were significantly more compliant than the thin matrices in compression ($P<0.05$, supplemental Figure ID) and shear (refer to supplemental methods). Despite degradation of the compliant matrices over the culture period, which reduced the overall thickness of these matrices to approximately 1.75 mm, the stiffness of both the thick and thin matrices remained constant (supplemental Figure II).

Proliferation and Morphological Changes

When cultured in complete medium without calcifying supplements, VICs proliferated more rapidly on compliant matrices ($P<0.05$; supplemental Figure IIIA), but the morphology was similar on the two matrices (Figure 1A and 1B). In contrast, VIC proliferation rate was not significantly different on stiff and compliant matrices when cultured in calcifying media (supplemental Figure IIIB), but morphological differences were substantial. In calcifying media, VICs on compliant matrices formed multicellular aggregates after 8 to 10 days of culture (Figure 1C). In contrast, VICs on stiff matrices formed fewer aggregates ($P<0.05$) and instead tended to form ridges (Figure 1D and 1E). In medium without procalcific

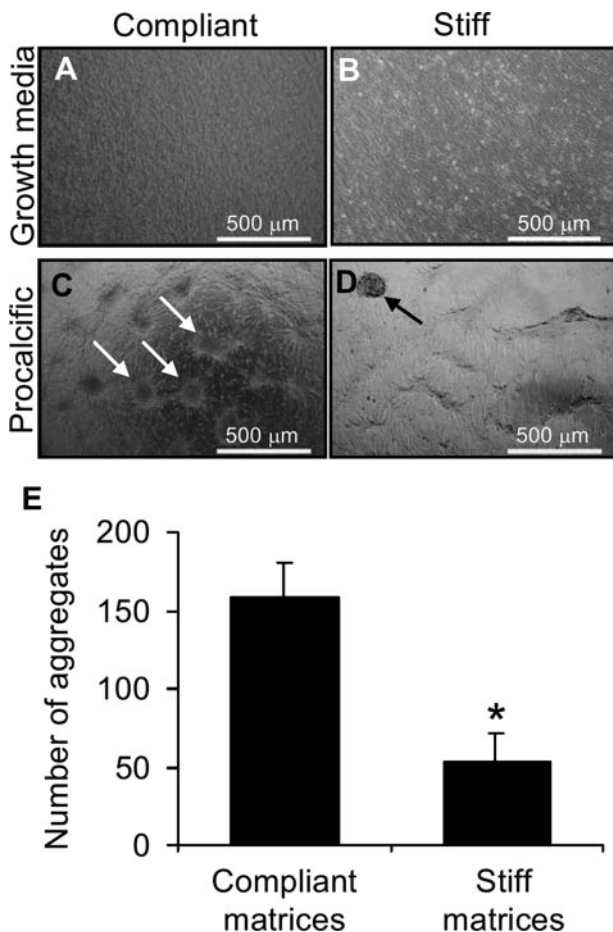


Figure 1. Cellular morphology. A through D, Bright field images of VICs cultured in DMEM or in calcifying media, with arrows indicating cell aggregates. E, Number of aggregates formed by VICs in media with osteogenic supplements on compliant and stiff matrices, * $P < 0.05$.

supplements, there was no aggregation on either substrate over the culture period.

More Compliant Matrices Promote Osteogenic Differentiation of VICs

VICs can form aggregates in vitro that contain calcium deposits and osteoblast-related proteins,⁷ so we investigated whether this was the case for the cell aggregates on compliant and stiff collagen matrices. There was a trend for greater calcification on the compliant matrices ($P < 0.06$; Figure 2A). Calcium deposition was localized within the aggregates formed on both matrices (supplemental Figure IV). Transcriptional expression of osteonectin and osteocalcin were significantly higher in VICs cultured on compliant matrices ($P < 0.05$ for osteonectin; $P < 0.06$ for osteocalcin; Figure 2B), as were protein expression of Runx2 ($P < 0.05$; Figure 2C), ALP activity (Figure 2D), and osteocalcin protein expression (Figure 2F). ALP activity and osteocalcin expression were localized within the aggregates on compliant matrices. On stiff substrates, ALP activity was weak and dispersed throughout the cell layer (Figure 2E) and minimal osteocalcin expression was observed, even in aggregates (Figure 2G).

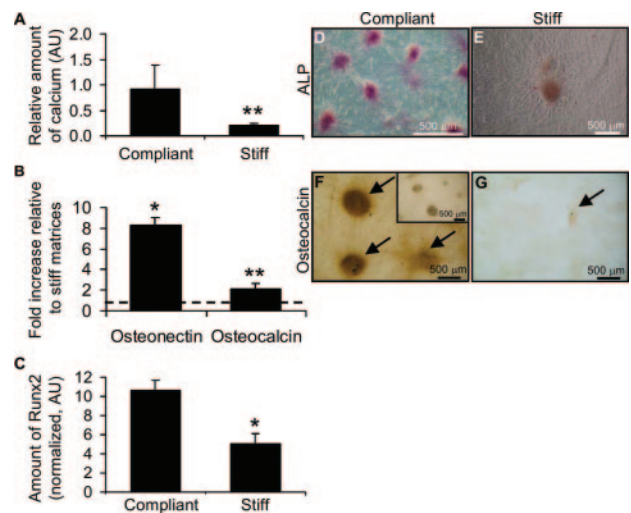


Figure 2. Compliant matrices promote osteogenic phenotypes. A, Relative amount of calcium, ** $P = 0.06$. B, Relative gene expression of osteocalcin and osteonectin by VICs, * $P < 0.05$ and ** $P = 0.06$. C, Runx2 expression, * $P < 0.05$. D and E, ALP staining. F and G, Osteocalcin expression, inset showing negative control.

Stiffer Matrices Promote Calcification Through Apoptosis

Although VICs on stiff matrices expressed osteoblast-related markers at low levels, significant calcium deposition was observed within the few aggregates that formed. Morphological analysis by SEM revealed significant differences in the spreading and shape of the cells on the surface of and around the multicellular aggregates on the 2 matrices (Figure 3A and 3B), which suggested that the aggregates formed and calcified through different mechanisms on the 2 matrices. Both in vivo and in vitro, calcification can occur through a process involving apoptosis,^{11,15} so we examined cell viability in the aggregates. On compliant matrices, the aggregates contained viable cells with little evidence of apoptosis (Figure 3C and 3E). Positive calcein AM staining was not attributable to the presence of calcium, as formalin-fixed calcified aggregates stained negatively (Figure 3C, inset). In contrast, aggregates formed on stiff matrices contained dead and apoptotic cells (Figure 3D and 3F).

Aggregate Formation on Stiffer Matrices Is Mediated by Cytoskeletal Tension

The striking differences in VIC phenotypes, aggregate morphology, and calcification process on compliant versus stiff matrices in otherwise identical culture conditions suggested that VICs sense and respond to matrix stiffness. Stiff culture surfaces, such as tissue culture polystyrene, are known to promote myofibrogenic differentiation of VICs and increase expression of filamentous α -SMA,¹⁹ a cytoskeletal protein that contributes to the contractility of activated VICs. We found that VICs displayed F-actin fibers regardless of matrix stiffness (supplemental Figure V). However, VICs on compliant matrices expressed predominantly monomeric α -SMA, whereas abundant expression of filamentous α -SMA was observed only in cells cultured on stiff matrices (Figure 4A and 4B) consistent with the emergence of a myofibroblast

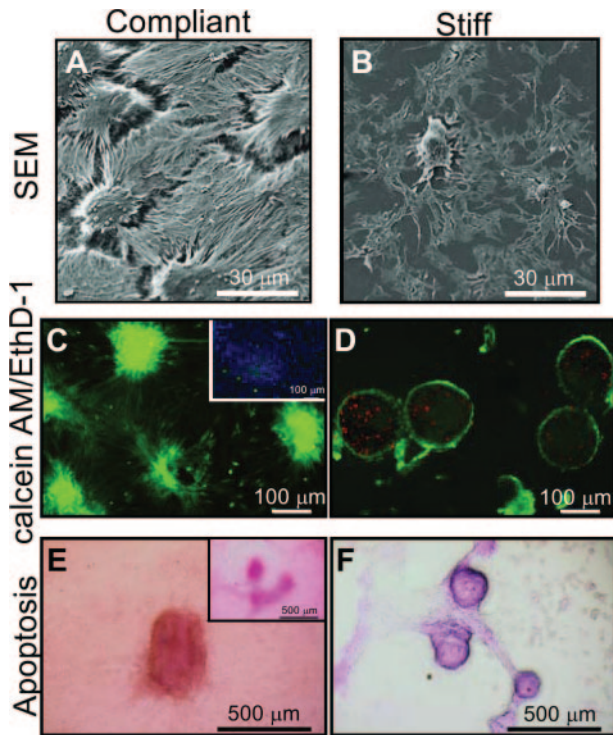


Figure 3. Stiffer matrices promote calcification associated with VIC apoptosis. A and B, SEM of cell aggregates. C and D, Live (green) and dead (red) staining of aggregates, inset showing the negative control with nuclear counterstaining (blue). E and F, APOPercentage staining for apoptosis, inset showing positive control (purple).

phenotype. We investigated the role of actin assembly in matrix stiffness-dependent aggregate formation by disrupting actin filaments in VICs. Actin depolymerization was observed in VICs after 48 hours of SWA treatment on both matrices (Figure 4C and 4D). Cells remained attached to the matrices; some were rounded with limited extension of cytoplasmic processes (Figure 4G and 4H). On compliant matrices, actin disruption had no effect on the formation of cell aggregates that displayed osteogenic phenotypes (Figure 4G). In contrast, on stiff matrices disruption of actin assembly significantly reduced the formation of aggregates ($P < 0.05$; Figure 4H and 4I). These data, along with the “contracted” appearance of the aggregates formed on the stiff matrices (Figure 3B), suggested that apoptosis leading to calcification on stiff substrates may be attributable to local contraction of the cell layer resulting from increased cytoskeletal tension, which is then released on aggregation. To test this, we released constrained collagen gels seeded with VICs and observed a significant increase in the number of apoptotic cells (Figure 5A). Previous studies have identified the Akt signaling pathway as the mediator of contraction-dependent apoptosis.²⁵ We found that Akt activation was downregulated on gel contraction by VICs (Figure 5B), before apoptosis, suggesting mechanically-regulated Akt activity influences apoptosis in VICs.

VIC Response to TGF- β and the Expression of its Receptors Are Matrix Stiffness-Dependent

TGF- β 1 is a potent inducer of α -SMA expression and myofibroblast differentiation. It is also expressed in calcified aortic

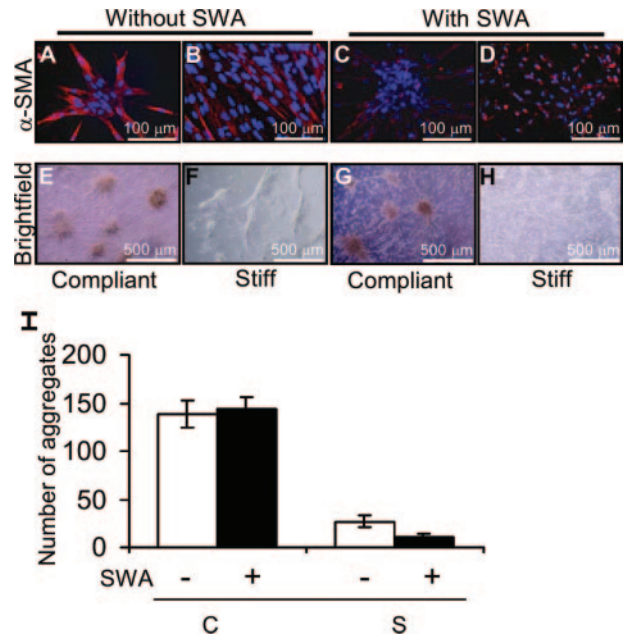


Figure 4. Matrix stiffness-dependent involvement of the actin cytoskeleton in aggregate formation. A through D, α -SMA expression (red) by VICs (nuclei, blue) without and with SWA. E through H, Brightfield images of VICs before and after SWA treatment, showing the absence of aggregates or ridges on the stiff matrices on SWA treatment. I, SWA affects aggregate formation by VICs, $*P < 0.05$.

valves¹⁵ and promotes VIC apoptosis and calcified aggregate formation in vitro.^{7,15} We evaluated whether matrix stiffness-dependent aggregation was influenced by TGF- β 1. No differences were detected in endogenous total TGF- β 1 production by VICs on compliant versus stiff matrices (data not shown). After only 5 days of culture, aggregates formed on stiff matrices treated with 5 ng/mL exogenous TGF- β 1 (28 ± 4 aggregates), but not without TGF- β 1 (zero aggregates; $P < 0.05$). In contrast, no aggregates were observed after 5 days on compliant matrices in the absence or presence of TGF- β 1. VICs grown in calcifying media for 8 days on either substrate had significantly lower expression of both TGF- β 1 receptor I and II compared with freshly isolated VICs ($P < 0.05$; supplemental Figure VI). Whereas TGF- β receptor II expression was not different on compliant versus stiff matrices, TGF- β receptor I expression was significantly lower in VICs on compliant matrices ($P < 0.05$; supplemental Figure VI). These data suggest that the preferential responsiveness to TGF- β 1 on stiff matrices is mediated in part through matrix stiffness-dependent expression of TGF- β receptor I.

Discussion

VICs,⁷ vascular smooth muscle cells,²⁶ and pericytes²⁷ can be induced in vitro to form aggregates that are typically referred to as calcified nodules. The mechanisms by which VICs form calcified aggregates and the factors that regulate these processes are not well defined. Here, we demonstrated 2 distinct calcification processes that are mechanically regulated and associated with different cell phenotypes. VICs cultured in calcifying media on more compliant matrices were viable, acquired osteoblast-like properties, and formed calcified

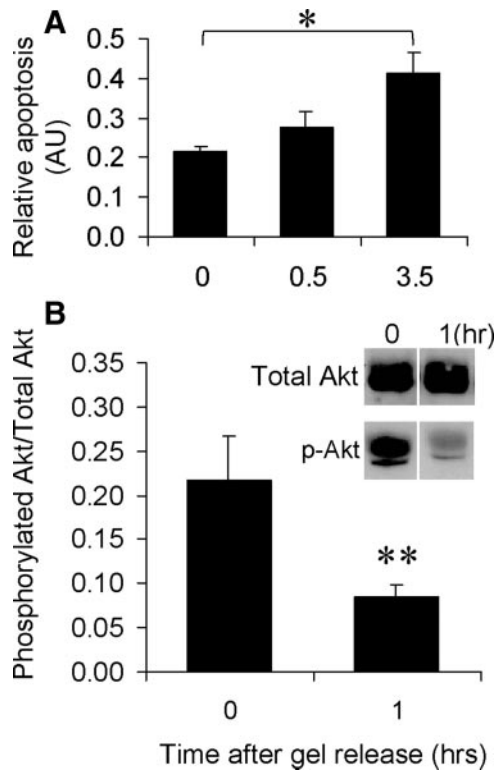


Figure 5. Contraction-induced apoptosis involving Akt signaling. A, Apoptosis determined by APOPercentage dye on release of constrained collagen gels, $*P < 0.05$. B, Western blot of total Akt and phosphorylated Akt (p-Akt) in cells on gels before release and 1 hour after release, $**P = 0.06$.

bone-like nodules. In contrast, VICs cultured in the same media but on the stiffer matrices had minimal osteoblast marker expression, differentiated to contractile myofibroblasts, and formed calcified aggregates containing apoptotic cells. Importantly, calcification on either matrix occurred within the culture duration only when the VICs were exposed to calcifying medium. Thus, matrix stiffness alone was insufficient to cause calcification but worked in conjunction with soluble factors to regulate VIC differentiation and calcification.

The experimental system used here permitted specific investigation of distinct calcification mechanisms; this has not been possible to date and has been largely ignored, confounding interpretation of cell culture data and limiting our understanding of the mechanisms underlying calcification by VICs. We used primary VICs to capture the heterogeneity of VICs in intact valves^{2,28} and to avoid the phenotypic changes that occur with subculture, including myofibroblast differentiation¹⁹ and loss of osteoprogenitors.²⁹ Cells were grown on fibrillar type I collagen gels instead of monomeric collagen-coated synthetic gels³⁰ to better mimic the native ECM in heart valves. This may be important as different intracellular signaling pathways are activated when cells bind fibrillar versus monomeric collagen.^{31,32} Although the compliant and stiff matrices were biochemically identical initially, changes in matrix composition attributable to cell remodeling may have occurred with time in culture. Calcification by valvular and vascular cells is similar on collagen-

and fibronectin-coated substrates,^{33,34} suggesting that replacement of collagen with fibronectin during remodeling would not elicit the differences observed in the current study. The effect of other matrix components produced by VICs on calcification is unknown, and thus characterization of the compositional changes that occur in the gels because of remodeling would better define the relative contributions of matrix stiffness versus composition. To manipulate only matrix stiffness, we were limited to a 2D system, as decoupling of matrix mechanics and chemistry is not possible with 3D fibrillar collagen matrices.³⁰ Based on previous studies,^{35,36} some VIC responses are similar in 3D matrices as on 2D surfaces, but 3D matrix stiffness effects on VIC differentiation have yet to be studied.

Based on Hertz contact analysis of microindentation data of collagen gels identical to those used here,³⁷ the apparent elastic moduli of the thick and thin collagen matrices are estimated to be 27 kPa and 113 kPa, respectively. Of note, VICs underwent osteogenic differentiation in the same stiffness range (25 to 40 kPa) as bone marrow-derived MSCs,³⁸ consistent with recent evidence that the aortic valve also contains a subpopulation of MSCs with robust osteogenic calcification potential.²⁹

The differentiation of VICs to contractile myofibroblasts that express filamentous α -SMA on stiff substrates has been reported previously.¹⁹ The primary inducers of myofibroblast differentiation are mechanical tension and TGF- β .³⁹ Cytoskeletal tension is generated intrinsically by cells as they exert tractional forces on the surrounding extracellular matrix; stiff matrices provide greater resistance to deformation, resulting in greater tractional forces.¹⁸ The incorporation of α -SMA into stress fibers aids in force generation.⁴⁰ We found that α -SMA stress fibers were critical to aggregation on stiffer matrices, as this process was inhibited by treatment with SWA, which disrupts polymerization of α -SMA,⁴¹ and was promoted by TGF- β 1. The dependency of aggregation on cytoskeletal tension, along with the appearance of ridges and the final symmetrical morphology of the aggregates suggested that the aggregates formed by local contraction of the cell layer. Release of mechanical tension in VICs, as would occur with contraction-induced aggregation, reduced Akt activity and subsequently triggered apoptosis as it does in other myofibroblasts.^{24,25,42} Apoptosis is associated with calcification of vascular and valvular cells in vitro⁴³ and in vivo,^{11,44} and is required for TGF- β 1-induced calcification by VICs.¹⁵ Our observations suggest a mechanically-based mechanism with which to interpret in vitro models of apoptosis-associated VIC calcification, particularly those performed on stiff polystyrene tissue culture plates that induce myofibroblast differentiation.¹⁹ This mechanism is also likely to be important in vivo where increases in myofibroblasts,^{19,45} apoptotic cells,¹¹ and TGF- β 1¹⁵ are observed in sclerotic leaflets and alterations in matrix tension are believed to be a trigger for myofibroblast apoptosis during wound repair.^{24,42}

In contrast to stiff matrices, addition of exogenous TGF- β 1 did not accelerate calcification on compliant substrates. The relative insensitivity of the cells on the compliant matrices to TGF- β 1 likely resulted from lower expression of the TGF- β receptor I. Fibroblasts are less sensitive to TGF- β when

grown in 3D spheroids than when grown as 2D monolayers on glass.⁴⁶ The differential responsiveness was reported to correlate with downregulation of TGF- β receptor expression in 3D culture, which in light of our findings, may reflect differences in effective matrix mechanical properties between 2D and 3D culture systems. We also observed significant downregulation of both TGF- β receptor I and II transcripts in VICs grown under calcifying conditions on either substrate compared to those freshly isolated from normal valves. This is consistent with observations from explanted human aortic valves, in which these receptors were downregulated in calcified leaflets relative to noncalcified leaflets.¹⁵

Although our findings have clear implications for the interpretation of VIC calcification in vitro and for the selection of biomaterials for valve regeneration, the relevance to valve calcification in vivo remains to be determined. Similar to atherosclerosis, AS is an active pathobiological process that involves extensive matrix remodeling.^{5,47,48} The extracellular matrix provides biochemical and mechanical cues to adherent cells, and alterations in the composition^{47,49} and mechanical properties²⁰ of the ECM are characteristic of sclerotic diseases. The effects of matrix composition on calcification have been reported,^{33,34,50} but the influence of matrix stiffness on vascular or valvular calcification has not been investigated. Notably, changes in the local stiffness of atherosclerotic lesions occur early, before substantial histological changes in the matrix.²⁰ Similar early dynamic changes in matrix mechanics are expected in sclerotic valves, but the alterations in the micromechanical stiffness of the valve matrix that occur with disease progression and the factors that contribute to these mechanical changes have yet to be determined. Although the collagen gels used here are far less complex than valve tissue in composition and structure, the modulus of the stiffer gels was comparable to that of sclerotic valve tissue (based on relative changes from normal tissue²¹) and the modulus of the more compliant gels was approximately 2- to 3-fold greater than the micromechanical tensile modulus of normal aortic valve tissue,⁵¹ but similar to that of early atherosclerotic lesions.²⁰ The matrices that mimicked the normal or early disease stiffness promoted osteogenic differentiation when the cells were exposed to calcific soluble signals, consistent with the appearance of osteoblast-like VICs early in AS⁴⁵ before the substantial matrix changes and calcification that ultimately stiffen the matrix. Although these findings are intriguing, further investigation is required to determine the role of matrix stiffness in modulating osteogenic and nonosteogenic calcification processes in vivo. In particular, translation of these findings to valve disease requires additional studies of the dynamic temporal and spatial changes that occur in matrix structure and composition during disease development and their relationships to the micromechanical properties of the valve matrix and cell phenotypes.

In summary, our data demonstrate that the differentiation of VICs and calcification in response to biochemical factors are modulated by the mechanical properties of the matrix. These data suggest an important regulatory role for matrix mechanics in valve cell biology, with implications for the interpretation of in vitro models of VIC calcification, the

selection of biomaterials for tissue engineered heart valves, and possibly disease development. Although we observed that either osteogenic or myofibroblastic differentiation of VICs can result in calcification in vitro, the two processes are distinct and respectively mimic aspects of either bone formation or apoptosis-associated calcification in vivo. The identification of distinct calcification processes suggests the need for therapies that are specific, yet capable of targeting multiple pathways involved in VIC pathological differentiation and valve calcification.

Acknowledgments

We thank Stephanie Ting, Zahra Mirzaei, Justin Parreno, Jian Wang, and Robert Chernenko for expert technical assistance.

Sources of Funding

This work was supported by a Grant-in-Aid (NA 6047) from the Heart and Stroke Foundation of Ontario, the Natural Sciences and Engineering Research Council of Canada, the Canada Research Chair in Mechanobiology (to C.A.S.), the Ontario Early Researcher Award (to C.A.S.), and a Heart and Stroke Richard Lewar Centre of Excellence Studentship (to C.Y.Y.Y.).

Disclosures

None.

References

- Chester AH, Taylor PM. Molecular and functional characteristics of heart-valve interstitial cells. *Philos Trans R Soc Lond B Biol Sci.* 2007; 362:1437–1443.
- Liu AC, Joag VR, Gotlieb AI. The emerging role of valve interstitial cell phenotypes in regulating heart valve pathobiology. *Am J Pathol.* 2007; 171:1407–1418.
- Stewart BF, Siscovick D, Lind BK, Gardin JM, Gottdiener JS, Smith VE, Kitzman DW, Otto CM. Clinical factors associated with calcific aortic valve disease. Cardiovascular Health Study. *J Am Coll Cardiol.* 1997;29: 630–634.
- Mohler ER III, Gannon F, Reynolds C, Zimmerman R, Keane MG, Kaplan FS. Bone formation and inflammation in cardiac valves. *Circulation.* 2001;103:1522–1528.
- O'Brien KD. Pathogenesis of calcific aortic valve disease: a disease process comes of age (and a good deal more). *Arterioscler Thromb Vasc Biol.* 2006;26:1721–1728.
- Otto CM, Lind BK, Kitzman DW, Gersh BJ, Siscovick DS. Association of aortic-valve sclerosis with cardiovascular mortality and morbidity in the elderly. *N Engl J Med.* 1999;341:142–147.
- Mohler ER III, Chawla MK, Chang AW, Vyavahare N, Levy RJ, Graham L, Gannon FH. Identification and characterization of calcifying valve cells from human and canine aortic valves. *J Heart Valve Dis.* 1999;8: 254–260.
- Speer MY, Giachelli CM. Regulation of cardiovascular calcification. *Cardiovasc Pathol.* 2004;13:63–70.
- Mohler ER III. Mechanisms of aortic valve calcification. *Am J Cardiol.* 2004;94:1396–1402, A1396.
- Tanaka K, Sata M, Fukuda D, Suematsu Y, Motomura N, Takamoto S, Hirata Y, Nagai R. Age-associated aortic stenosis in apolipoprotein E-deficient mice. *J Am Coll Cardiol.* 2005;46:134–141.
- Rajamannan NM, Sangiorgi G, Springett M, Arnold K, Mohacs T, Spagnoli LG, Edwards WD, Tajik AJ, Schwartz RS. Experimental hypercholesterolemia induces apoptosis in the aortic valve. *J Heart Valve Dis.* 2001;10:371–374.
- Filip DA, Nistor A, Bulla A, Radu A, Lupu F, Simionescu M. Cellular events in the development of valvular atherosclerotic lesions induced by experimental hypercholesterolemia. *Atherosclerosis.* 1987;67:199–214.
- Rajamannan NM, Subramaniam M, Rickard D, Stock SR, Donovan J, Springett M, Orszulak T, Fullerton DA, Tajik AJ, Bonow RO, Spelsberg T. Human aortic valve calcification is associated with an osteoblast phenotype. *Circulation.* 2003;107:2181–2184.
- Clark-Greuel JN, Connolly JM, Sorichillo E, Narula NR, Rapoport HS, Mohler ER III, Gorman JH III, Gorman RC, Levy RJ. Transforming

- growth factor-beta1 mechanisms in aortic valve calcification: increased alkaline phosphatase and related events. *Ann Thorac Surg*. 2007;83:946–953.
15. Jian B, Narula N, Li QY, Mohler ER III, Levy RJ. Progression of aortic valve stenosis: TGF-beta1 is present in calcified aortic valve cusps and promotes aortic valve interstitial cell calcification via apoptosis. *Ann Thorac Surg*. 2003;75:457–465; discussion 465–456.
 16. Mathieu P, Voisine P, Pepin A, Shetty R, Savard N, Dagenais F. Calcification of human valve interstitial cells is dependent on alkaline phosphatase activity. *J Heart Valve Dis*. 2005;14:353–357.
 17. Osman L, Yacoub MH, Latif N, Amrani M, Chester AH. Role of human valve interstitial cells in valve calcification and their response to atorvastatin. *Circulation*. 2006;114:1547–552.
 18. Discher DE, Janney P, Wang YL. Tissue cells feel and respond to the stiffness of their substrate. *Science*. 2005;310:1139–1143.
 19. Pho M, Lee W, Watt DR, Laschinger C, Simmons CA, McCulloch CA. Cofilin is a marker of myofibroblast differentiation in cells from porcine aortic cardiac valves. *Am J Physiol Heart Circ Physiol*. 2008;294:H1767–H1778.
 20. Matsumoto T, Abe H, Ohashi T, Kato Y, Sato M. Local elastic modulus of atherosclerotic lesions of rabbit thoracic aortas measured by pipette aspiration method. *Physiol Meas*. 2002;23:635–648.
 21. Imanaka K, Takamoto S, Ohtsuka T, Oka T, Furuse A, Omata S. The stiffness of normal and abnormal mitral valves. *Ann Thorac Cardiovasc Surg*. 2007;13:178–184.
 22. Bellows CG, Melcher AH, Aubin JE. Contraction and organization of collagen gels by cells cultured from periodontal ligament, gingiva and bone suggest functional differences between cell types. *J Cell Sci*. 1981;50:299–314.
 23. Gregory CA, Gunn WG, Peister A, Prockop DJ. An Alizarin red-based assay of mineralization by adherent cells in culture: comparison with cetylpyridinium chloride extraction. *Anal Biochem*. 2004;329:77–84.
 24. Grinnell F, Zhu M, Carlson MA, Abrams JM. Release of mechanical tension triggers apoptosis of human fibroblasts in a model of regressing granulation tissue. *Exp Cell Res*. 1999;248:608–619.
 25. Xia H, Nho RS, Kahm J, Kleidon J, Henke CA. Focal adhesion kinase is upstream of phosphatidylinositol 3-kinase/Akt in regulating fibroblast survival in response to contraction of type I collagen matrices via a beta 1 integrin viability signaling pathway. *J Biol Chem*. 2004;279:33024–33034.
 26. Watson KE, Bostrom K, Ravindranath R, Lam T, Norton B, Demer LL. TGF-beta 1 and 25-hydroxycholesterol stimulate osteoblast-like vascular cells to calcify. *J Clin Invest*. 1994;93:2106–2113.
 27. Canfield AE, Doherty MJ, Wood AC, Farrington C, Ashton B, Begum N, Harvey B, Poole A, Grant ME, Boot-Handford RP. Role of pericytes in vascular calcification: a review. *Z Kardiol*. 2000;89 Suppl 2:20–27.
 28. Schoen FJ. Evolving concepts of cardiac valve dynamics: the continuum of development, functional structure, pathobiology, and tissue engineering. *Circulation*. 2008;118:1864–1880.
 29. Chen J-H, Yip CYY, Sone ED, Simmons CA. Identification and characterization of aortic valve mesenchymal progenitor cells with robust osteogenic calcification potential. *Am J Pathol*. 2009;174:1109–1119.
 30. Yip CYY, Chen J-H, Simmons CA. Engineering substrate mechanics to regulate cell response. In: Khademhosseini A, Borenstein J, Toner M, Takayama S, eds. *Micro- and Nanoengineering of the Cell Microenvironment: Technologies and Applications*. Norwood, Mass: Artech House; 2008.
 31. Koyama H, Raines EW, Bornfeldt KE, Roberts JM, Ross R. Fibrillar collagen inhibits arterial smooth muscle proliferation through regulation of Cdk2 inhibitors. *Cell*. 1996;87:1069–1078.
 32. Nishiyama T, Horii I, Nakayama Y, Ozawa T, Hayashi T. A distinct characteristic of the quiescent state of human dermal fibroblasts in contracted collagen gel as revealed by no response to epidermal growth factor alone, but a positive growth response to a combination of the growth factor and saikosaponin b1. *Matrix*. 1990;10:412–419.
 33. Rodriguez KJ, Masters KS. Regulation of valvular interstitial cell calcification by components of the extracellular matrix. *J Biomed Mater Res A*. In press.
 34. Watson KE, Parhami F, Shin V, Demer LL. Fibronectin and collagen I matrixes promote calcification of vascular cells in vitro, whereas collagen IV matrix is inhibitory. *Arterioscler Thromb Vasc Biol*. 1998;18:1964–1971.
 35. Shah DN, Recktenwall-Work SM, Anseth KS. The effect of bioactive hydrogels on the secretion of extracellular matrix molecules by valvular interstitial cells. *Biomaterials*. 2008;29:2060–2072.
 36. Monzack EL, Gu X, Masters KS. Efficacy of simvastatin treatment of valvular interstitial cells varies with the extracellular environment. *Arterioscler Thromb Vasc Biol*. 2009;29:246–253.
 37. Arora PD, McCulloch CA. Dependence of collagen remodelling on alpha-smooth muscle actin expression by fibroblasts. *J Cell Physiol*. 1994;159:161–175.
 38. Engler AJ, Sen S, Sweeney HL, Discher DE. Matrix elasticity directs stem cell lineage specification. *Cell*. 2006;126:677–689.
 39. Tomasek JJ, Gabbiani G, Hinz B, Chaponnier C, Brown RA. Myofibroblasts and mechano-regulation of connective tissue remodelling. *Nat Rev Mol Cell Biol*. 2002;3:349–363.
 40. Hinz B, Celetta G, Tomasek JJ, Gabbiani G, Chaponnier C. Alpha-smooth muscle actin expression upregulates fibroblast contractile activity. *Mol Biol Cell*. 2001;12:2730–2741.
 41. Wang J, Fan J, Laschinger C, Arora PD, Kapus A, Seth A, McCulloch CA. Smooth muscle actin determines mechanical force-induced p38 activation. *J Biol Chem*. 2005;280:7273–7284.
 42. Tian B, Lessan K, Kahm J, Kleidon J, Henke C. beta 1 integrin regulates fibroblast viability during collagen matrix contraction through a phosphatidylinositol 3-kinase/Akt/protein kinase B signaling pathway. *J Biol Chem*. 2002;277:24667–24675.
 43. Proudfoot D, Skepper JN, Hegyi L, Bennett MR, Shanahan CM, Weissberg PL. Apoptosis regulates human vascular calcification in vitro: evidence for initiation of vascular calcification by apoptotic bodies. *Circ Res*. 2000;87:1055–1062.
 44. Clarke MC, Littlewood TD, Figg N, Maguire JJ, Davenport AP, Goddard M, Bennett MR. Chronic apoptosis of vascular smooth muscle cells accelerates atherosclerosis and promotes calcification and medial degeneration. *Circ Res*. 2008;102:1529–1538.
 45. Aikawa E, Nahrendorf M, Sosnovik D, Lok VM, Jaffer FA, Aikawa M, Weissleder R. Multimodality molecular imaging identifies proteolytic and osteogenic activities in early aortic valve disease. *Circulation*. 2007;115:377–386.
 46. Kunz-Schughart LA, Wenninger S, Neumeier T, Seidl P, Knuechel R. Three-dimensional tissue structure affects sensitivity of fibroblasts to TGF-beta 1. *Am J Physiol Cell Physiol*. 2003;284:C209–C219.
 47. Hinton RB Jr, Lincoln J, Deutsch GH, Osinska H, Manning PB, Benson DW, Yutzey KE. Extracellular matrix remodeling and organization in developing and diseased aortic valves. *Circ Res*. 2006;98:1431–1438.
 48. Fondard O, Detant D, Jung B, Choqueux C, Adle-Biassette H, Jarraya M, Hvass U, Couetil JP, Henin D, Michel JB, Vahanian A, Jacob MP. Extracellular matrix remodelling in human aortic valve disease: the role of matrix metalloproteinases and their tissue inhibitors. *Eur Heart J*. 2005;26:1333–1341.
 49. McDonald TO, Gerrity RG, Jen C, Chen HJ, Wark K, Wight TN, Chait A, O'Brien KD. Diabetes and arterial extracellular matrix changes in a porcine model of atherosclerosis. *J Histochem Cytochem*. 2007;55:1149–1157.
 50. Simionescu A, Simionescu DT, Vyavahare NR. Osteogenic responses in fibroblasts activated by elastin degradation products and transforming growth factor-beta1: role of myofibroblasts in vascular calcification. *Am J Pathol*. 2007;171:116–123.
 51. Vesely I, Noseworthy R. Micromechanics of the fibrosa and the ventricularis in aortic valve leaflets. *J Biomech*. 1992;25:101–113.

Supplement material

Calcification by valve interstitial cells is regulated by the stiffness of the extracellular matrix

Cindy Ying Yin Yip, Jan-Hung Chen, Ruogang Zhao, Craig A. Simmons

Institute of Biomaterials and Biomedical Engineering, Cardiovascular Sciences Collaborative Program, Department of Mechanical and Industrial Engineering, and Faculty of Dentistry
University of Toronto, Toronto, ON, Canada

Correspondence to: Craig Simmons (c.simmons@utoronto.ca)

Detailed materials and methods

Unless otherwise stated, all reagents were purchased from Sigma-Aldrich (Oakville, ON, Canada).

Valve interstitial cell isolation and culture. Hearts were obtained from 8 month old pigs immediately after death (Quality Meat Packers, Toronto, ON). Pig hearts were immediately stored in ice-cold phosphate buffered saline (PBS) containing calcium and magnesium and transported to the laboratory for dissection and cell isolation. Aortic valve leaflets were excised and were rinsed in sterile PBS containing 0.5% (vol/vol) of amphotericin B, 10,000 Units/mL penicillin, and 10 mg/mL streptomycin. To remove endothelial cells, leaflets were pre-digested with collagenase (150 units/mL) reconstituted in N-Tris(hydroxymethyl)methyl-2-aminoethanesulfonic acid (TES) buffer with 0.36 mM calcium chloride (pH=7.4) for 20 minutes at 37°C and then for seven additional minutes at 37°C with 0.125% trypsin and EDTA. Leaflets were then vortexed and lightly scraped with sterile rubber policemen on both surfaces to remove all endothelial cells. The valve leaflets were rinsed with PBS, minced and further digested by collagenase reconstituted in PBS (150 units/mL) for an additional two hours at 37°C. To facilitate the release of interstitial cells from valve matrix, digested leaflets were vortexed and the cell suspension was collected by removing undigested tissue pieces with a cell strainer. An equal volume of complete medium (consisting of Dulbecco's modified Eagle's medium (DMEM) with 10% fetal bovine serum (FBS; Hyclone, Logan, UT), 10,000 Units/mL penicillin, and 10 mg/mL streptomycin) and cell suspension was mixed and centrifuged at $284 \times g$ for seven minutes. Supernatant was removed and the cells were resuspended in complete medium. Cell viability and total cell number were counted by a Vi-Cell™ cell viability analyzer (Beckman Coulter, Mississauga, ON, Canada). Cells were subsequently seeded on constrained collagen matrices at 10,000 cells/cm² and were incubated for eight to ten days at 37°C, 5% CO₂ in either complete medium, or in calcifying medium consisting of complete medium with 10 mM β-glycerophosphate, 10 μg/mL ascorbic acid and 10 nM dexamethasone.

Preparation of collagen matrices. Fresh collagen solutions were prepared for each experiments and prepared as described previously¹. A mixture with the following chemicals was prepared on

ice: (1) 0.3 mL 10X concentrated DMEM; (2) 0.3 mL 0.25M NaHCO₃ buffer; (3) 0.3 mL FBS; (4) 0.3 mL penicillin/streptomycin mixture; (5) 0.12 mL 0.1 M NaOH buffer; and (6) 2.5 mL bovine collagen (PureCol, Inamed Biomaterials, Fremont, CA). For thick collagen matrices, 500 µl of collagen mixture was pipetted into each well of a 24-well microtiter plate lined with sterile coverslips. Polymerization of collagen was achieved by incubating the collagen mixture at 37 °C in a 5% CO₂ incubator overnight. To make thin collagen matrices, the same volume of collagen mixture was applied to the surface of the well and the coverslips for one minute at room temperature. Excess collagen mixture was then removed by aspiration, leaving a thin collagen coating in the well that was polymerized overnight.

Scanning electron microscopy. Compliant and stiff collagen matrices with or without cells were evaluated by scanning electron microscopy. Samples were fixed with 4% formaldehyde, followed by dehydration in a series of ethanol washes at 30%, 50%, 70%, 95% and 100% ethanol for 30 minutes each. Samples were then critical point dried with liquid carbon dioxide in a Polaron CPD7501, mounted on SEM aluminum stubs and sputter coated with gold using a Polaron SC 515 SEM Coating System. The samples were examined at 1,000X to 5,000X magnification using a scanning electron microscope (Model S-2500, Hitachi Instrument). For collagen matrices without cells, images were used for estimating the collagen fibril diameters with ImageJ software (NIH, Bethesda, MD).

Characterization of the content and the mechanical properties of the collagen gels. The collagen content of the thick and thin matrices was measured by colorimetric hydroxyproline assay after zero, three and eight days in culture. Briefly, collagen matrices were papain digested, followed by release of hydroxyproline with acid hydrolysis using 6 N hydrochloride acid (HCL). The hydroxylate was then neutralized with 5.7 N sodium hydroxide. The extracted hydroxyproline was oxidized into a pyrrole with 0.05 N chloramines T, followed by treatment with 4-dimethylaminobenzaldehyde to develop a colour change. The amount of hydroxyproline was quantified by measuring the absorbance of the solution at 560 nm.

The effective stiffness of the initial collagen matrices (hydrated) as well as those cultured for three and eight days was measured in compression using a Biosyntech Mach-1 mechanical test system (Laval, QC). Constrained thick and thin gels (n = 4 of each) were compressed within 24-well culture plates using an 8 mm diameter loading platen. Load-displacement curves were recorded, from which the effective stiffness was determined as the initial tangential slope. Because the effective stiffness in this system is dictated in part by the geometry and boundary constraints of the gels in the wells, tensile stiffness could not be measured *in situ*.

To demonstrate the relative difference in the stiffness of the thick and thin collagen matrices under shear loading that better mimics the tractional forces applied by cells on the gels, we performed finite element (FE) analysis using ANSYS (Canonsburg, PA). Two-dimensional, plane strain FE models of the gels, representing a vertical slice through the thick and thin gels, were constructed. The thickness of the thick and thin collagen gels was set to the initial thickness of 2.5 mm and 10 µm, respectively, to mimic the experimental conditions. Eight-node elements were used to discretize the models. Collagen was modeled as a hyperelastic neo-Hookean material with shear modulus of 30 kPa. The gels were constrained in both the horizontal and

vertical directions on the left and bottom edges. The right edge of the models was left unconstrained to allow for measurement of the shear deformation.

To demonstrate the relative difference in shear deformation between the thick and thin gels, an arbitrary constant shear force of $0.48 \mu\text{N}/\text{mm}$ was applied to the top surface of both gels over the entire width of the model. The maximum shear displacement (at the top-right corner for both models) was $10.16 \mu\text{m}$ and $0.36 \mu\text{m}$ for the thick and thin gels, respectively. These results indicate that the effective stiffness of thick gels under shear forces was significantly less than that of the thin gels, as expected and consistent with the results from the compression tests.

Measurement of cell proliferation. Cells cultured on compliant or stiff matrices were rinsed with sterile PBS without calcium and magnesium. VICs were released from collagen matrices with collagenase digestion ($300 \text{ units}/\text{mL}$) for 1 hour at 37°C . Culture media, degraded collagen and collagenase solution were centrifuged at 4°C at $16200 \times g$ for 5 minutes, followed by aspiration of the supernatant. Cell pellets were rinsed with ice-cold PBS. Proliferation was determined at various time points based on measurement of DNA content of cell pellets via binding with fluorescent dye from the CyQUANT® NF cell proliferation assay kit (Invitrogen, Burlington, ON). To do so, cell pellets were resuspended and incubated with the dye for 1 hour at 37°C in a 96-well microtiter plate. The fluorescence intensity of each sample was measured using a microplate reader with excitation at 485 nm and emission detection at 530 nm. A standard curve consisting of 100 to 20,000 cells was generated with primary VICs to quantify the actual number of cells in the test samples.

Staining of viable, dead and apoptotic cells. VICs on compliant or stiff matrices were quickly rinsed with sterile PBS. Viable cells were determined by fluorescent labeling with $4 \mu\text{M}$ Calcein AM and dead cells were labeled with $2 \mu\text{M}$ Ethidium Homodimer-1 (LIVE/DEAD® Viability/Cytotoxicity Kit for mammalian cells, Invitrogen, Burlington, ON). Cells on gels were incubated with fluorescent dye for 1 hour at 37°C and then nuclei counterstained with Hoechst 33242 dye for 5 minutes. Samples were subsequently mounted on microscope slides with PermaFluor mounting medium and examined by fluorescence microscopy immediately (Olympus Model IX71). As a negative control, cells were killed by formalin fixation prior to Calcein AM staining and nuclear counterstaining to confirm that the Calcein AM staining was specific to viable cells and not simply binding calcium.

Apoptotic cells were identified by cellular uptake of APOPercentage™ dye (Biocolor Ltd, Carrickfergus, UK) as a result of apoptosis-induced membrane phosphatidylserine and phosphatidylcholine translocation. In brief, samples were quickly rinsed with sterile PBS with calcium and magnesium prior to incubation with APOPercentage™ dye diluted 1:20 in supplemented DMEM at 37°C for 30 minutes. Samples were then mounted on microscope slides with PermaMount aqueous mounting medium and images were captured under the microscope. Positive controls were achieved by chemically-induced apoptosis of cells using 5 mM hydrogen peroxide for 3 hours at 37°C prior to staining. Intense staining, typically bright pink or purple depending on the culture substrate and cell density, was observed in the positive controls, ensuring the validity of the apoptosis detection method in VICs. Negative controls were achieved by incubating samples without the APOPercentage™ dye.

Polymerase chain reaction for expression of osteogenic markers. VICs were released from collagen matrices via collagenase digestion (300 units/mL at 37°C for 1 hour). Cell pellets were obtained by centrifugation, followed by aspiration of the supernatant. Total RNA was isolated from cell pellets following standard protocols of the Micro RNeasy System (Qiagen, Mississauga, ON). Subsequently, total RNA was reverse transcribed with oligo-(dT)₁₂₋₁₈ primers (Invitrogen) and Superscript III reverse transcriptase (Invitrogen). cDNA was quantified with a NanoDrop Spectrophotometer (ND-1000, NanoDrop Technologies, Wilmington, DE), and then used as the template for real-time PCR using SYBR Green, an annealing temperature of 60°C, and 35 cycles. Two osteoblast-related transcripts, osteonectin (Accession number: AW436132, forward primers: 5'-tccggatctttccttgctttcta-3' and reverse primer 5'-ccttcacatcgtggcaagagtttg-3') and osteocalcin (Accession number: AW346755, forward primers: 5'-tcaaccccgactgcgacgag-3' and reverse primer 5'-ttggagcagctgggatgatgg-3') were tested². Glyceraldehyde-3-phosphate dehydrogenase (Accession number: AF017079, forward primers: 5'-tgtaccaccaactgcttggc-3' and reverse primer 5'-ggcatggactgtggtcatgag-3') was used as the housekeeping gene³. Transcriptional expression was quantified by the comparative Ct (Cycle threshold) method ($2^{-\Delta\Delta Ct}$ method) with the following equations:

$$\Delta Ct = Ct \text{ of target gene} - Ct \text{ of housekeeping gene} \quad (\text{Equation 1})$$

$$\Delta\Delta Ct = \Delta Ct_{\text{Compliant matrices}} - \Delta Ct_{\text{Stiff matrices}} \quad (\text{Equation 2})$$

$$\text{fold increase between two matrices} = 2^{-\Delta\Delta Ct} \quad (\text{Equation 3})$$

Measurement of core binding factor alpha-1 (cbfa-1) protein. Cbfa-1 protein expression was measured using a commercially-available ELISA-based immunoassay (TransAM kit, ActiveMotif, Carlsbad, CA). Nuclear extracts were prepared from VICs following the manufacturer's recommendations. Briefly, VICs were released from collagen matrices with collagenase digestion (as described above) and cell pellets were obtained. Samples were then rinsed with ice-cold PBS with phosphatase inhibitor buffer (125 mM sodium fluoride, 250 mM β -glycerophosphate, 250 mM para-nitrophenyl phosphate and 25 Mm sodium vanadate) to prevent inactivation of cbfa-1. Pellets were resuspended in ice-cold hypotonic buffer (20 mM HEPES, 5 mM sodium fluoride, 10 μ M sodium thioglycolate and 0.1 M EDTA) and allowed to swell on ice for 15 minutes. Cell membranes were disrupted by gentle mixing with 10% Igepal CA-630, followed by centrifugation. Nuclear pellets were resuspended in Complete Lysis Buffer (1 M DTT, protease inhibitor cocktail, lysis buffer AM4) and rocked gently on ice for 30 minutes. Nuclear extract was obtained by collecting the supernatant upon centrifugation.

The protein concentration in the nuclear extract was determined using a micro BCA assay (Pierce, Rockford, IL). For each sample, 20 μ g of nuclear extract was used to measure the abundance of cbfa-1 by an ELISA-based immunoassay following the recommended protocol. Briefly, nuclear extracts containing unknown amount of activated transcription factor were incubated for 1 hour in 96-well microtiter plates pre-coated with oligonucleotides containing an AML-3 consensus binding site. Primary antibody for AML-3/Runx2 (cbfa-1) was added to the samples for another one hour incubation, followed by one hour incubation with horseradish peroxidase-conjugated anti-rabbit IgG. The colorimetric reaction was initiated by five minute incubation with the Developing Solution, followed by the Stop Solution. Absorbance of each sample was read immediately with a spectrophotometer at 450 nm with a reference wavelength of 655 nm. Absorbance readings were normalized by total cell number per sample. A positive

control for AML-3/Runx2 activation was performed with 5 $\mu\text{g}/\text{well}$ of Saos-2 nuclear extract. Negative controls were achieved with blank compliant and stiff collagen gels without any cells.

Alkaline phosphatase and Alizarin Red S staining. To stain for alkaline phosphatase activity (ALP), VICs on collagen matrices were fixed in 10% neutral buffered formalin (NBF) and rinsed in distilled water. Samples were stained using Naphthol AS MX-PO₄ (Fisher Scientific, Ottawa, ON) as the substrate, N,N-Dimethylformamide, Trizma-hydrochloride acid, and Fast Red Violet LB salt. The stained samples were rinsed with distilled water three times and examined under a light microscope. Positively stained cells display a redish/purple color. To detect the presence of calcium salts, formalin fixed samples were washed with distilled water, followed by staining with 0.02 mg/mL Alizarin red S (ARS) solution. Cells with calcium deposition were stained bright red. Subsequently, ARS dye was released from the stained samples using 0.6 N HCl, followed by neutralization with 10% (vol/vol) ammonium hydroxide. The amount of released dye was quantified by measuring the absorbance of the extracted dye in solution at 405 nm.

Osteocalcin immunohistochemical staining. Immunohistochemical staining for osteocalcin was performed using Vectastain Universal Elite ABC Kit (Vector Laboratories, Burlingame, CA). Samples were fixed in 10% NBF and washed with 0.05% Tween 20 in PBS. Following fixation, samples were treated with 3% hydrogen peroxide in methanol at room temperature for 10 minutes, blocked with horse serum for 20 minutes at room temperature, and then incubated for three hours at room temperature with 20 $\mu\text{g}/\text{mL}$ mouse anti-bovine osteocalcin antibody (clone OCG4; Affinity BioReagents, Golden, CO) diluted in 0.3% Triton X-100 in PBS. Secondary biotinylated antibody and 3,3'-diaminobenzidine (DAB) substrate were then applied. The stained samples were dehydrated in an ethanol gradient. Negative controls were achieved by omitting the primary antibody.

Immunofluorescence staining of cytoskeletal proteins. VICs on collagen matrices were fixed in 10% NBF, followed by permeabilization with 0.1% Triton-X and rinsing with PBS. Samples were blocked with 3% bovine serum albumin to minimize non-specific binding. To stain for α -smooth muscle actin (α -SMA), monoclonal mouse anti- α -SMA antibody (1:100 dilution; Clone 1A4) and Alexa Fluor® 568 goat anti-mouse antibody (1:100 dilution) were used. Filamentous (F)-actin was stained by fluorescein isothiocyanate (FITC)-conjugated phalloidin (1:100 dilution). Nuclei were stained with Hoechst 33242 dye (1:1000 dilution). Samples were mounted on microscope slides with PermaFluor and were examined under a fluorescence microscope (Model IX71, Olympus, Center Valley, PA).

Disruption of actin cytoskeleton. VICs were treated with 0.4 nM of Swinholide A (SWA) after six days of culture on compliant or stiff matrices in calcifying media. Medium with fresh SWA was exchanged every 24 hours for two days. After two days of treatment with SWA, expression of α -SMA and F-actin were analyzed with immunostaining and the number of aggregates was recorded.

Response to TGF- β 1. In a separate set of experiments, VICs were cultured on compliant and stiff matrices and were immediately treated with calcifying media (containing 10% FBS) and 5 ng/mL of TGF- β 1 for five days to induce SMA expression. The FBS used in these experiments was reported by the manufacturer to contain 10-22 ng/mL TGF- β (equivalent to 1-2.2 ng/mL in

the calcifying media). We attempted to reduce the baseline TGF- β 1 concentration in the media by using 1% FBS, but this resulted in a significant reduction in proliferation and no formation of calcified aggregates after up to 10 days on both compliant and stiff matrices, even with the addition of exogenous TGF- β 1. Responsiveness of VICs to TGF- β 1 was also determined by measuring the transcript expression of TGF- β 1 receptor I and II by RT-PCR using the following primers sequence: (1) TGF- β 1 receptor I, accession number: AB182260.1, forward primers: 5'-gacggcattccagtggttct-3' and reverse primer 5'-tgcacatacaaatggcctgt-3') and (2) TGF- β 1 receptor II, accession number: EF396957.1, forward primers: 5'-cagggagaacgttcaggt-3' and reverse primer 5'-ccaaccaagctgagtcacat-3').

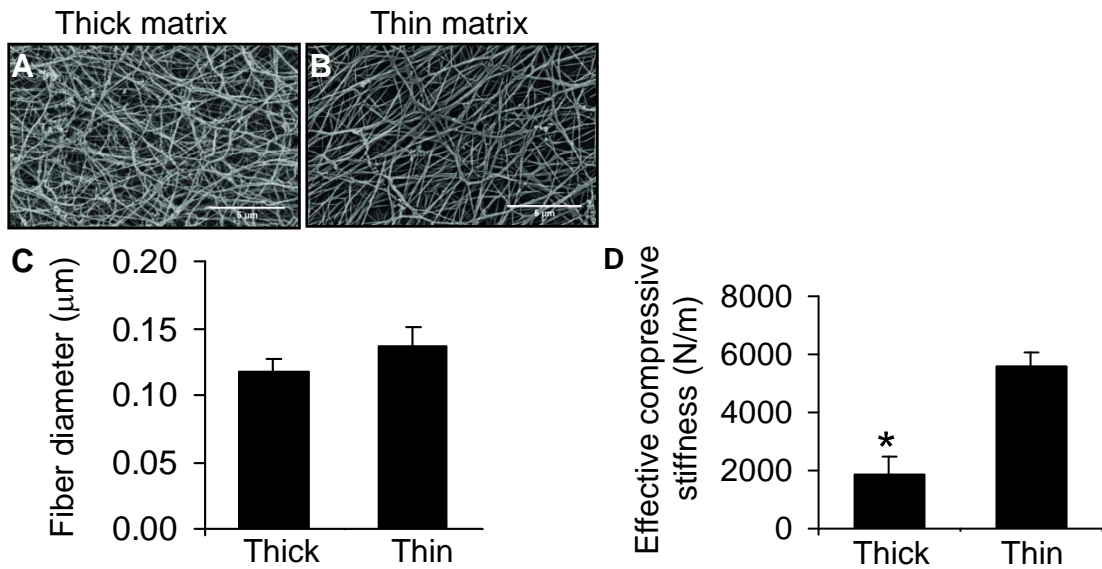
Transforming growth factor (TGF)- β 1 expression. VICs were grown on compliant or stiff matrices for eight days, with media changes every two days. 48 hour conditioned media was collected on the last day of culture. TGF- β 1 in the conditioned media was measured using the TGF- β 1 Emax® ImmunoAssay System (Promega, Nepean, ON) according to the manufacturer's directions. Briefly, TGF- β 1 coat monoclonal antibody, which binds to soluble TGF- β 1, was adhered to the surface of a 96-well microtiter plate. Samples for generating the standard curve and the test samples were applied to each pre-coated well. Samples were incubated with anti-TGF- β 1 polyclonal antibody, followed by incubation with a species-specific antibody conjugated to horseradish peroxidase. Colorimetric development was achieved by the addition of TMB One solution. The reaction was stopped by 1 N hydrochloric acid. Absorbance was read at 450 nm on a plate reader and then normalized by total cell number per sample.

Contraction-dependent apoptosis. VICs were cultured on constrained collagen gels for six days with osteogenic media at a cell density of 10,000 cells/cm². Cellular contraction was induced by releasing the gels from the walls of the culture wells. Cells were stained with APOPercentageTM dye after 0, 0.5, and 3 hours of gel release to detect the presence of apoptosis. The level of apoptosis was quantified colorimetrically (absorbance at 550 nm) upon dye release. In a separate experiment using the same culture methodology, proteins were extracted from cells after 0 and 1 hour of gel release, followed by western blot for the detection of total Akt and phosphorylated Akt.

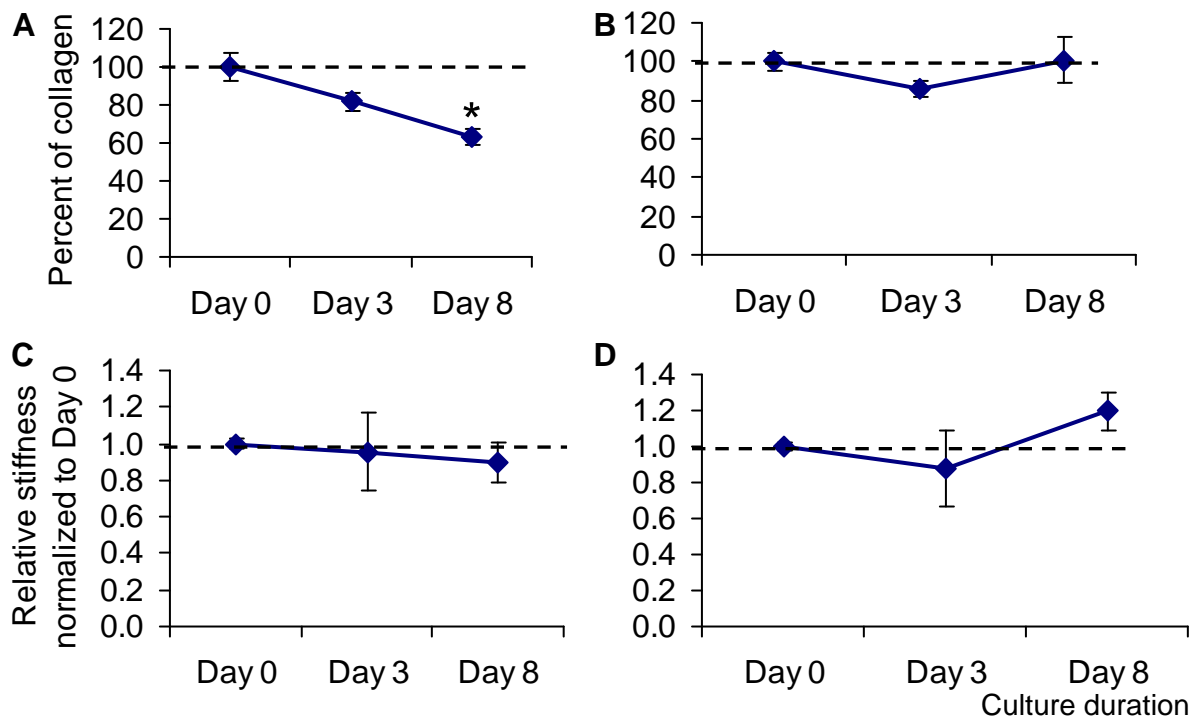
Statistical analysis. Results are presented as mean \pm standard error. Unpaired Student's *t*-test was used for comparisons between two groups. ANOVA and Fisher's least significant difference test were used to evaluate statistical significant differences in multiple group comparisons.

References:

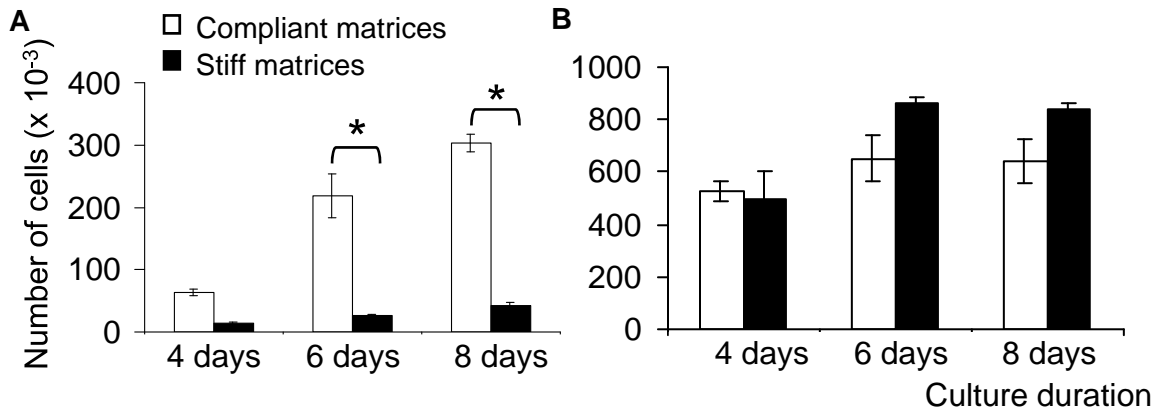
1. Bellows CG, Melcher AH, Aubin JE. Contraction and organization of collagen gels by cells cultured from periodontal ligament, gingiva and bone suggest functional differences between cell types. *J Cell Sci.* 1981;50:299-314.
2. Ringe J, Kaps C, Schmitt B, Buscher K, Bartel J, Smolian H, Schultz O, Burmester GR, Haupl T, Sittlinger M. Porcine mesenchymal stem cells. Induction of distinct mesenchymal cell lineages. *Cell and Tissue Research.* 2002;307(3):321-327.
3. Chai H, Zhou W, Lin P, Lumsden A, Yao Q, Chen C. Ginsenosides block HIV protease inhibitor ritonavir-induced vascular dysfunction of porcine coronary arteries. *American Journal of Physiology.* 2005;288(6):H2965-2971.



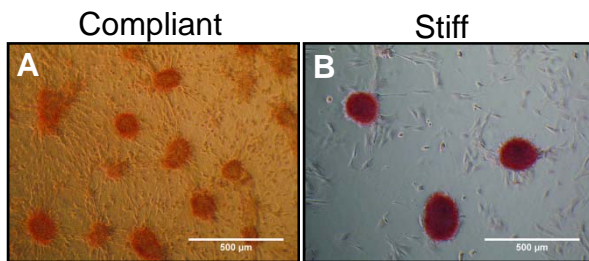
Supplemental Figure I. *Characterization of collagen matrices.* SEM images of thick (A) and thin (B) collagen matrices. (C) Comparison of fibril diameters. (D) Initial effective stiffness of collagen matrices in compression, * $P < 0.05$.



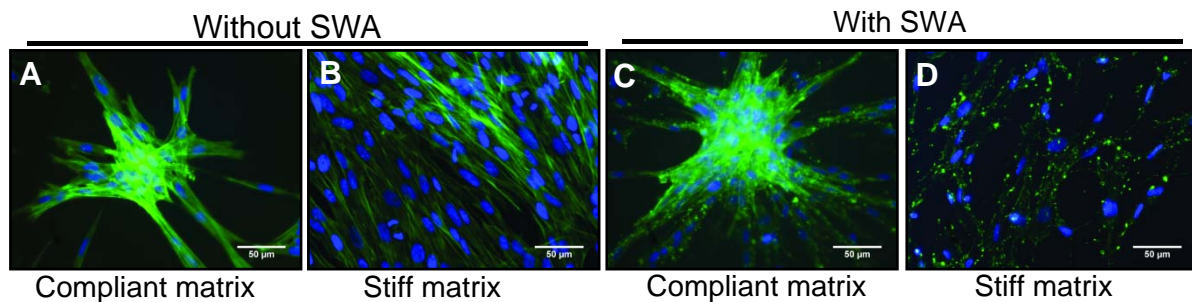
Supplemental Figure II. *Characterization of the collagen content and the stiffness of the matrices over the course of cell culture.* (A,B) Data were expressed as percentage of collagen remaining relative to day 0. (A) Significant collagen degradation was observed in compliant matrices after eight days of culture (* $P < 0.05$, compared to gels from day 0 and day 3). (B) Content of collagen remained relatively constant for the stiff matrices. Stiffness of compliant matrices (C) and stiff matrices (D) did not change significantly over the culture duration.



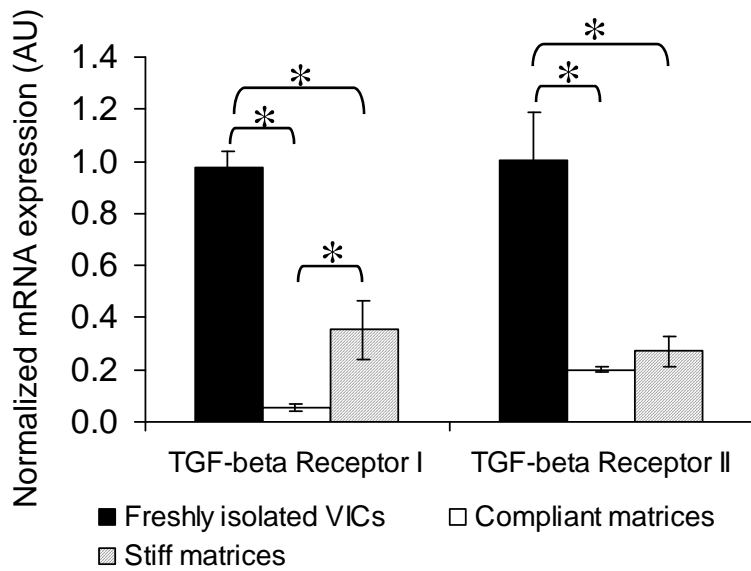
Supplemental Figure III. Cellular proliferation. Proliferation of VICs in DMEM (A), and calcifying media (B) after eight days in culture, * $P < 0.05$.



Supplemental Figure IV. ARS staining for calcium expression on compliant (A) and stiff (B) matrices.



Supplemental Figure V. F-actin expression. Expression of F-actin (green) by VICs (nuclei counterstained blue) without SWA treatment (A) and after SWA treatment (B).



Supplemental Figure VI. Transcript expression of TGF- β receptors I and II in healthy, freshly isolated VICs as well as in VICs cultured on compliant and stiff matrices, * $P < 0.05$.